fermentation

MDPI

Article

Immobilization of Phospholipase D for Production of Phosphatidylserine via Enzyme-Inorganic Hybrid Nanoflower Strategy

Shujing Zhang, Hui Sun, Zhiqi Huang, Zhuoxuan Han, Jiayi Hou, Fuping Lu and Yihan Liu *

Key Laboratory of Industrial Fermentation Microbiology, Ministry of Education, Tianjin Key Laboratory of Industrial Microbiology, College of Biotechnology, Tianjin University of Science and Technology, Tianjin 300457, China; zsjtust@163.com (S.Z.); huisun26@163.com (H.S.); hhuangzhiqi@163.com (Z.H.); zxhan419@163.com (Z.H.); houjiayi0618@126.com (J.H.); lfp@tust.edu.cn (F.L.)

* Correspondence: lyh@tust.edu.cn

Abstract: Phosphatidylserine (PS) is a natural phospholipid with particular importance in the food, cosmetic, and pharmaceutical industries. Recently, the synthesis of PS mediated by phospholipase D (PLD) has drawn great attention. But the application of free PLD is limited by various drawbacks, including its instability under extreme conditions, difficulties in reuse and recovery, and high costs. In this work, saPLD-inorganic hybrid nanoflowers (saPLD@NFs) were synthesized with PLD from *Streptomyces antibioticus* (saPLD) as the organic component and $Ca_3(PO_4)_2$ as the inorganic component. The saPLD@NFs demonstrated outstanding immobilization capability and achieved a 119% enzyme activity recovery rate. Furthermore, the saPLD@NFs exhibited better thermostability and pH stability in comparison to free saPLD. The PS yield of saPLD@NFs was about 57.4% in the first cycles and still reached 60.4% of its initial PS yield after four cycles. After 25 d storage at 4 °C, saPLD@NFs retained 66.5% of its original activity, but free saPLD only retained 38.3%, indicating that saPLD@NFs have excellent storage stability. Thus, this study established a new method of preparing PLD nanoflowers for effective PS synthesis, which might accelerate the practical utilization of this biocatalyst.

Keywords: phosphatidylserine; phospholipase D; immobilization; enzyme-inorganic hybrid nanoflowers

Citation: Zhang, S.; Sun, H.; Huang, Z.; Han, Z.; Hou, J.; Lu, F.; Liu, Y. Immobilization of Phospholipase D for Production of Phosphatidylserine via Enzyme-Inorganic Hybrid Nanoflower Strategy. *Fermentation* **2023**, *9*, 1016. https://doi.org/10.3390/fermentation9121016

Academic Editor: Ronnie G. Willaert

Received: 6 October 2023
Revised: 8 December 2023
Accepted: 11 December 2023
Published: 13 December 2023

1. Introduction

Phosphatidylserine (PS), as a type of natural phospholipid (PL), has been widely used in many applications, including the pharmaceutical and functional food sectors, due to its physicochemical properties [1–3]. Clinical studies have demonstrated that dietary intake of PS can be beneficial for children with attention deficit hyperactivity disorder, and it has an excellent influence on preventing or improving Alzheimer's disease [4]. Orally administrated PS can effectively break through the blood–brain barrier and safely slow, halt, or reverse the structural deterioration and biochemical alterations in the nerve cell membrane [5,6]. Additionally, PS can be utilized as an efficient sports nutrition supplement to reduce circulating cortisol concentrations, expedite recovery, and prevent muscle soreness during and after exercise [7], such as endurance running, weight training, and cycling.

The main approaches regarding preparing PS include the extraction and enzymatic methods. Extraction methods are primarily applied to extract PS from animals and plants. Animal organs including bovine brain are possible sources to obtain PS, which may not be appropriate for human consumption owing to the transmission risk of infectious diseases [8]. In addition, PS can be obtained from soybeans, vegetable oils, and yolk. But the high price of PS is caused by complex extraction and separation technology, the low availability, and high loss rate. Thus, it is critical to increase the PS yield to meet the demand. L-serine and phosphatidylcholine (PC) as substrates can be used to synthesize PS through a transphosphatidylation reaction of phospholipase D (PLD, EC 3.1.4.4) [9].

PC can be easily and simply acquired in large quantities from different natural materials, including soybean and egg, which are comparatively cheap for producing PC industrially. Comparing with the extraction methods, enzymatic synthesis of PS has drawn lots of attention owing to its mild reaction conditions, extensive range of substrate sources, and high reaction efficiency [10].

PLD belongs to the phosphodiesterase superfamily. It extensively exists in plants, animals, and microorganisms [11]. On the contrary, microbial PLDs, particularly those isolated from *Streptomyces* genus, demonstrate generally higher transphosphatidylation activity [12,13]. PLD can catalyze two kinds of reactions: (i) hydrolyzing PC to choline and phosphatidic acid (PA) through cleaving its phosphodiester bond and (ii) transferring the phosphatidic acid moiety to an acceptor alcohol. The transphosphatidylation reaction is beneficial for synthesizing natural PLs, such as PS, phosphatidylethanolamine, phosphatidylinositol, and phosphatidylglycerol [14–16].

So far, a high cost has been caused by the low yield of PLD and complicated purification steps, and the free enzymes are difficult to reuse due to the instability, limiting their use in industrial PS production. As a promising strategy, immobilizing enzymes on/in materials can overcome these limitations due to advantages, such as improved stability, convenient handling and recyclable use. Over the last few decades, immobilized enzymes have been prepared using novel materials, including polymer resins, hydrogels, carbon nanotubes, gold nanoparticles, ordered mesoporous silica, and magnetic nanoparticles, as supports [17–22]. Moreover, the performances of enzymes have been enhanced using lots of immobilization approaches, such as physical adsorption, encapsulation, covalent binding, and cross-linked enzyme aggregates [23–26]. However, most of the immobilized enzymes demonstrated lower activities than their free forms because of the improved diffusion resistance between substrate and enzyme and the change in enzyme conformation [27,28]. Therefore, it is a major challenge to simultaneously enhance the stability and activity of enzymes in the field of enzyme immobilization. Recently, the enzyme-inorganic hybrid nanoflowers strategy has been a rapidly developing field of materials chemistry due to the advanced designs with a specific structure and functionality [29]. Most importantly, enzyme-inorganic hybrid nanoflowers demonstrated higher activity, better stability, desirable reusability, and great potential in various applications in comparison to free enzymes [30].

Flower-like nanoparticles are formed by metal ions and protein in phosphate-buffered saline under mild conditions when using the enzyme-inorganic hybrid nanoflowers method. The formulation of enzyme-inorganic hybrid nanoflowers is composed of the nucleation and generation of primary crystals, further enlargement of the aggregates, and the entire generation of nanoflowers [31]. In the initial step, complexes are formed by protein molecules with metal ions, mainly via the coordination among the metal ion and nitrogen atoms of the amide groups existing in the protein backbone. The complexes can supply sites for nucleation. The anisotropic growth of nano-petals can be stipulated by the intramolecular interactions between the metal ion and protein. Proteins function as glue to bind the petals together, which consequently promotes the generation of a flower-like structure. So far, various enzymes, including catalase [32], lipase [33], trypsin [34], horseradish peroxidase [35], glucose oxidase [36], urease [37], laccase [38], soybean peroxidase [39], and papain [40], have been utilized to prepare enzyme-inorganic hybrid nanoflowers. For most of the enzymes, enzyme-inorganic hybrid nanoflowers can not only significantly enhance their activities but also increase their storage stability, reusability, and operational stability.

In this study, saPLD-inorganic hybrid nanoflowers (saPLD@NFs) were synthesized with $Ca_3(PO_4)_2$ as the inorganic component and PLD from *Streptomyces antibioticus* (saPLD) as the organic component, followed by determining the optimum immobilization conditions of saPLD. The thermostability and pH stability of saPLD@NFs and the free enzyme were studied and compared. In addition, the batch catalytic capacity and the catalytic reaction process parameters of saPLD@NFs in the synthesis of PS were further identified.

2. Materials and Methods

2.1. Materials and Reagents

Standard samples of PS (≥97%, from soybean) and PC (≥99%, from soybean) were provided by Sigma-Aldrich (St. Louis, MO, USA). Soybean lecithin (PC content ≥ 90%) was supplied by Yuanye Bio (Shanghai, China). L-serine was ordered from Solarbio Tech (Beijing, China). Calcium chloride anhydrous and propyl propionate were obtained from Macklin Biochemical Co., Ltd. (Shanghai, China). All other chemicals and reagents mentioned in this study were of analytical grade.

2.2. Preparation and Characterization of saPLD@NFs

First, saPLD was produced and purified according to the protocol reported by Mao et al. [41]. Then, saPLD@NFs were prepared with the simple wet-chemical precipitation method. Typically, $CaCl_2$ aqueous solution was added to 50 mM PBS buffer (pH 7.0) with 0.6 U of saPLD to a final concentration of 24 mM to prepare the saPLD@NFs in one pot. The resulting mixture was vortexed vigorously for 30 s and then incubated at 4 °C for 12 h. Subsequently, saPLD@NFs were pelleted by centrifugation for 2 min at 12,000 rpm. The saPLD@NFs were rinsed with ultrapure water thrice and dried using vacuum freeze-drying for further identification.

2.2.1. Scanning Electron Microscopy

The surface morphology of saPLD@NFs was detected using scanning electron microscopy Apreo (SEM, Thermo Fisher Scientific, Waltham, MA, USA). After depositing the dry saPLD@NFs on carbon-tape-covered stub, they were coated using gold source with a sputter coater before SEM operation. At last, images of saPLD@NFs were created using SEM.

2.2.2. Confocal Laser Scanning Microscopy

saPLD in 20 mM Tris-HCl buffer (pH = 7.0) was mixed with fluorescein isothiocyanate (FITC) dissolved in dimethyl sulfoxide, and the resultant solution was placed in the dark for 6 h with shaking at 300 rpm. The unbound FITC was eliminated by dialysis against distilled water. Then, confocal laser scanning microscopy was used to observe the saPLD labeled with FITC hybrid nanoflowers at excitation and emission wavelengths of about 495 nm/520 nm (CLSM; FV-1000 confocal microscope, Olympus, Tokyo, Japan).

2.2.3. Fourier-Transform Infrared Spectroscopy

Fourier-transform infrared spectroscopy (FT-IR) was utilized to identify the functional groups of saPLD@NFs and $Ca_3(PO_4)_2$. The measurements were conducted using the KBr pressed-pellet method. Each sample was measured with the FT-IR spectrophotometer (TENSOR, Bruker, Karlsruhe, Germany) in a range of 4000–400 cm^{-1} wavenumbers.

2.3. Measurements of saPLD@NFs and Free saPLD Activity

The transphosphatidylation activity of saPLD was determined by calculating the yield of PS from L-serine and PC. The reaction mixture was obtained by mixing 1 mL of 0.2 M sodium acetate buffer (pH 6.0) with 12 mg L-serine, 1.5 mL of propyl propionate with 25 mg PC, and 1 mL of saPLD or 1 g of saPLD@NFs. After 20 min incubation at 60 °C, 3 mL of chloroform/methanol (2:1, *v/v*) solution was used to extract the PS. Then, the mixture was centrifuged for 10 min at 12,000 rpm, and high-performance liquid chromatography (HPLC) was utilized to characterize the lower phase.

HPLC (Agilent Technologies, Palo Alto, CA, USA) analysis was carried out with a ZORBAX Rx-SIL silica gel column (5 μm, 4.6 × 250 mm, Agilent) connected to an ultraviolet detector. The mobile phase was acetonitrile/methanol/phosphoric acid (95:5:0.8, *v/v/v*) at a flow rate of 0.8 mL/min. In addition, the column was incubated at 25 °C, and the injection volume was 10 μL. The PS concentrations in samples were determined using the peak areas according to the standard curve obtained by injecting PS standards of known

concentrations (Figure S1). One unit of saPLD@NFs or free saPLD was designated as the quantity of enzyme producing 1 μmol of PS from PC per min.

2.4. Optimum Synthesis Conditions of saPLD@NFs

To detect the optimum synthesis conditions for saPLD@NFs, the concentration of calcium ions and the content of saPLD were optimized. Briefly, different concentrations of $CaCl_2$ solution were mixed with 50 mM PBS buffer (pH 7.0) with various contents of saPLD (0.15, 0.30, 0.45, 0.60, and 0.75 U), and the final concentrations of $CaCl_2$ were 12, 24, 36, and 48 mM, respectively. After vortexing vigorously for 30 s, the mixture was placed at 4 °C for 12 h. After incubation, the saPLD@NFs were centrifugally pelleted at 12,000 rpm for 2 min and rinsed three times with 2 mL of deionized water to eliminate the unfixed enzyme.

The optimum immobilization conditions to prepare saPLD@NFs were determined by the enzyme activity recovery rate and the relative enzyme activity. Generally, the enzyme activity recovery rate of saPLD@NFs was defined as the observed activity of immobilized enzymes divided by the total initial activity. The relative enzyme activity was the percentage of the enzyme activity to the maximum enzyme activity (Table S1).

2.5. Enzymatic Properties of saPLD@NFs

To determine the optimum temperature of saPLD@NFs and free saPLD, the reactions were performed at different temperatures (30, 40, 50, 60, 70, and 80 °C), and the enzyme activity was detected while keeping other conditions unchanged (Table S2). To study and compare the thermostability of saPLD@NFs and free saPLD, they were pre-incubated at differing temperatures (30, 40, 50, and 60 °C) in the absence of substrate for 1 h, respectively, and then the residual activity was monitored under standard assay conditions (Table S3).

To identify the optimum pH of saPLD@NFs and free saPLD, their activities were determined with the standard assay in a pH range of 5.0–9.0 by placing the reaction mixtures at 60 °C (Table S4). To determine the pH stability, saPLD@NFs and free saPLD samples were pre-incubated at 4 °C and different pH (5.0, 6.0, 7.0, and 8.0) for 7 d without substrate, and the residual activity was estimated under standard assay conditions (Table S5).

2.6. Preparation of PS via Enzymatic Method

PS synthesis was conducted in a two-phase reaction system. The oil phase was 3.0 mL of propyl propionate with 50 mg PC, and the aqueous phase was 2.0 mL of acetate/acetic acid buffer (0.2 M, pH 6.0) with 25 mg L-serine. Then, saPLD@NFs with various enzyme amounts (0.25, 0.50, and 0.75 g) were added, and the reaction was performed by oscillating with 200 rpm at 40 °C for differing times (1, 2, 3, 4, and 5 h), respectively. PS was extracted by mixing the reaction mixture with the solutions of chloroform/methanol (2:1, *v/v*). After centrifugation at 12,000 rpm for 10 min, the lower layer was harvested and characterized with HPLC, as noted in the "Measurements of saPLD@NFs and Free saPLD Activity" section. The PS conversion rate (mol%) was described as the PS yield, which was determined by the following equation: PS yield (mol%) = PS amount/initial PC amount × 100% (Table S6).

2.7. Storage Stability of saPLD@NFs

To study the storage stability, saPLD@NFs and free saPLD were incubated at 4 °C for 25 d in 20 mM Tris-HCl buffer (pH = 7.0), and the residual activity of saPLD@NFs and free saPLD was monitored at a specific time interval (every five days) under standard assay conditions.

2.8. Operational Stability of saPLD@NFs

In each reaction cycle, 0.45 g saPLD@NFs were used to catalyze the reaction containing 25 mg L-serine (in 2 mL of 0.2 M acetate/acetic acid buffer (pH = 6.0)) and 50 mg PC (in 3 mL of propyl propionate) at 40 °C for 3 h. To evaluate the operational stability of saPLD@NFs, they were immediately eliminated from the solution at the end of each reaction

by centrifugation (12,000 rpm, 2 min), rinsed thrice with Tris-HCl buffer (20 mM, pH = 7.0), and then reutilized in the new batch of reaction under the same reaction conditions. In addition, the operational stability for each batch cycle was identified by determining the relative PS yield in comparison to that of the initial reaction.

3. Results

3.1. Characterization of saPLD@NFs

Enzyme-inorganic hybrid nanoflowers with delicate structures of sepals and petals could be a new immobilized enzyme strategy. Figure 1 illustrates the general scheme of saPLD-inorganic hybrid nanoflower (saPLD@NFs) synthesis. At the early nucleation stage, complexes were generated by saPLD with calcium ions, mainly via the coordination of the metal ion and nitrogen atoms of amide groups in the enzyme backbone, which supplied a space for the nucleation of initial crystals. At the following growth stage, more crystals bound together and formed larger agglomerates, generating loose petal-like structures. At the last self-assembly stage, saPLD functioned as a scaffold to combine petals together into the nanoflower.

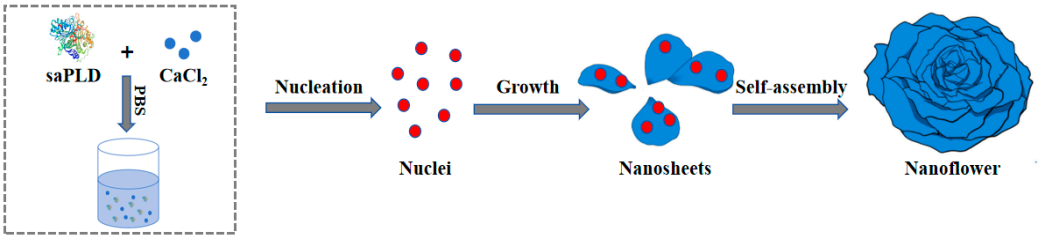

Figure 1. Schematic diagram of the formation of saPLD@NFs.

SEM was used to determine the general morphologies of saPLD@NFs. As demonstrated in Figure 2a, the low-resolution SEM images exhibited that saPLD@NFs comprised interconnected petals. The high-resolution SEM image (Figure 2b) demonstrated that hundreds of nanoplates assembled the hybrid nanoflowers, exhibiting a flower-like porous nanostructure with high surface-to-volume ratio. Furthermore, the CLSM image (Figure 2c) indicated the effective immobilization of saPLD in enzyme-inorganic hybrid nanoflowers due to the strong green fluorescence of saPLD labeled with fluorescein isothiocyanate (FITC). In addition, saPLD@NFs and $Ca_3(PO_4)_2$ were analyzed using FTIR spectroscopy. As shown in Figure 2d, in the spectra of $Ca_3(PO_4)_2$ and saPLD@NFs, the strong IR band at 1031 cm^{-1} was characteristic of P-O stretches and vibrations, while the bands at 563 cm^{-1} and 603 cm^{-1} might be due to the bending vibrations of bridging phosphorous including O=P-O, suggesting the presence of phosphate groups. Moreover, the characteristic peaks of saPLD@NFs at 1546 cm^{-1} corresponded to amide in the enzymes, indicating the existence of saPLD. Two groups of broad bands in the range of 1620–1660 and 3700–3200 cm^{-1} resulted from the presence of water in the spectra of $Ca_3(PO_4)_2$ and saPLD@NFs [42]. All the above results verified the successful synthesis of saPLD@NFs.

3.2. Effects of Preparation Conditions on the saPLD@NFs Activity

The synthesis steps of saPLD@NFs included nucleation, further growth, and final assembly of the flower-like structure. However, the nucleation step plays an important role in the further growth and final generation of enzyme-inorganic hybrid nanoflowers. The enzyme functions as a 'glue' to keep the metal phosphate nanocrystals together. Hence, the enzyme content has a remarkable influence on the nucleation number and assembly degree of enzyme-inorganic hybrid nanoflowers. Furthermore, the primary crystals of $Ca_3(PO_4)_2$ are generated at the early growth stage and then predominantly embedded with enzyme via the coordination of amide groups in the enzyme backbone. These complexes supply a space for the nucleation of the primary crystal. Thus, the concentration of Ca^{2+} is also critical, because it is a chief driving force for initiating the generation of nanocrystals and

further growth process. To acquire the optimal immobilization conditions of saPLD, the influence of enzyme content and Ca^{2+} concentration was studied.

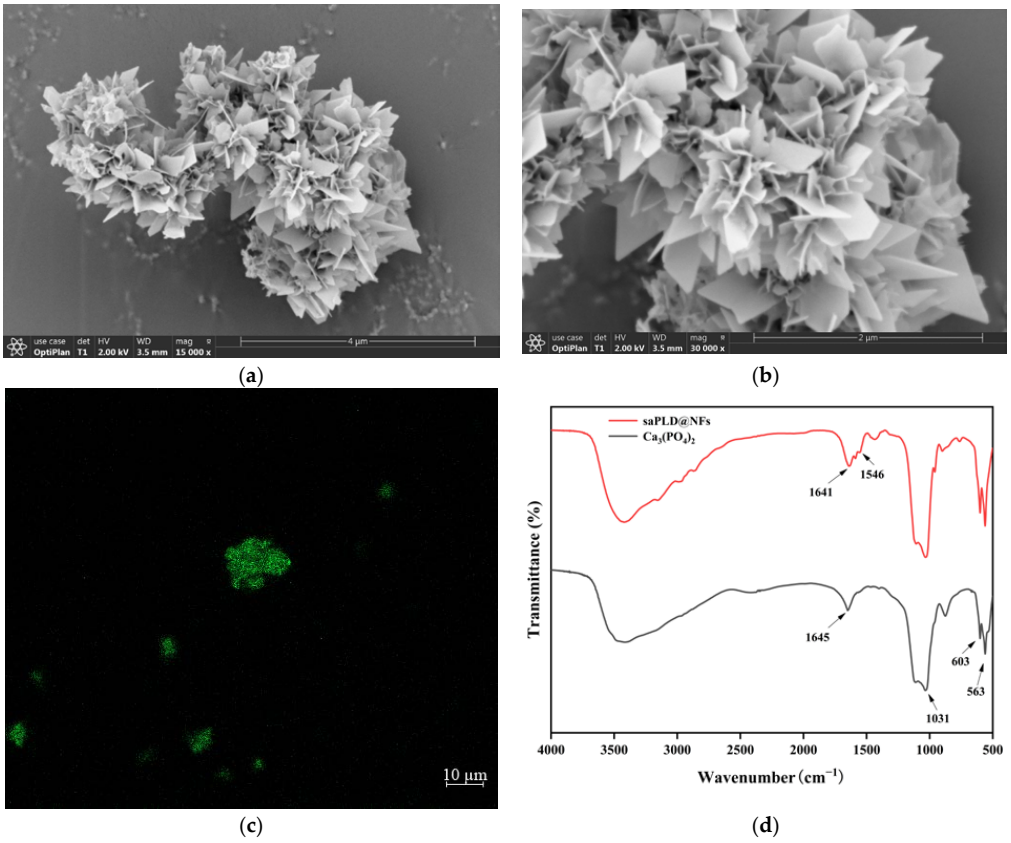

Figure 2. Characterization of saPLD@NFs. (**a**) SEM images of saPLD@NFs at 15,000× magnification; (**b**) SEM images of saPLD@NFs at 30,000× magnification; (**c**) CLSM image of saPLD@NFs; (**d**) FT-IR spectra of saPLD@NFs and $Ca_3(PO_4)_2$.

As indicated in Figure 3a,b, it was discovered that the relative enzyme activity and enzyme activity recovery rate of saPLD@NFs increased with the rising enzyme content (0.15 U–0.45 U). However, a further enhancement in enzyme content (>0.45 U) led to reduced relative enzyme activity and enzyme activity recovery rate of the saPLD@NFs. A possible reason could be the higher number of nucleation sites generated for $Ca_3(PO_4)_2$ nanocrystals due to the increased enzyme content. However, the capacity of the $Ca_3(PO_4)_2$ in the system would be reduced by too many enzymes, and steric hindrance could be introduced to the catalytic sites of saPLD by the tighter structures of nanoflowers with higher enzyme content. In addition, the increasing Ca^{2+} concentration (12 mM–36 mM) enhanced the relative enzyme activity and the enzyme activity recovery rate of saPLD@NFs at a certain enzyme concentration (Figure 3a,b). A possible explanation for this phenomenon is the fact that a lower concentration of Ca^{2+} was insufficient to reach the supersaturation point for initiating nucleation and succeeding growth of $Ca_3(PO_4)_2$ nanocrystals. Excessive Ca^{2+} concentration might lead to the compact structure of hybrid nanoflowers, which reduced the contact efficiency between saPLD and substrates, resulting in reduced enzyme activity. Moreover, when the saPLD@NFs were synthesized using 0.45 U enzyme amount and 36 mM Ca^{2+} concentration, saPLD@NFs demonstrated the highest recovery enzyme activity of 119%. Comparing to the free saPLD, the increased activity of saPLD in nanoflowers might be due to the following factors: (i) the favorable enzyme conformation in hybrid nanoflowers; (ii) the cooperative effect of nanoscale-entrapped saPLD molecules; (iii) the large surface area of saPLD@NFs that alleviated the mass-transfer limitations. In fact, Ca^{2+} also played a positive role in regulating the enzymatic activity for saPLD. In light of these

results, an enzyme amount of 0.45 U and Ca^{2+} concentration of 36 mM were chosen as the optimum conditions for preparing saPLD@NFs.

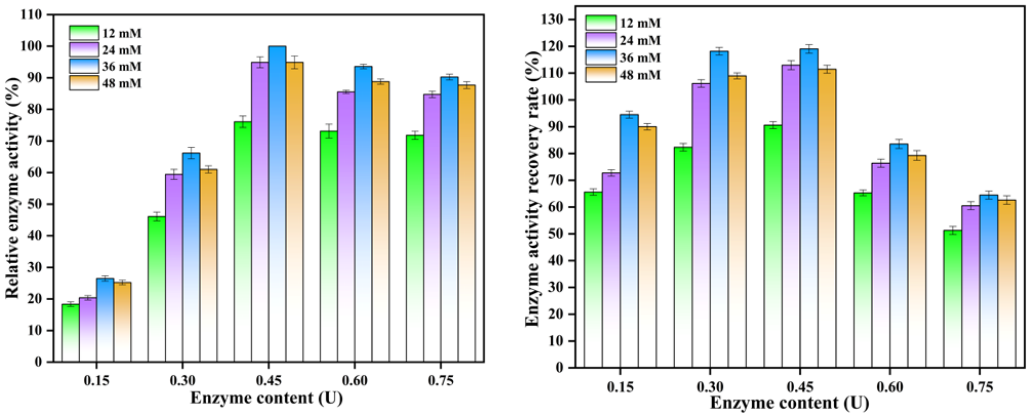

(**a**) (**b**)

Figure 3. The influence of enzyme content and Ca^{2+} concentration on the relative enzyme activity (**a**) and the enzyme activity recovery rate (**b**). The data exhibited are the average values obtained from three paralleled experiments, while the error bars stand for the standard deviations.

3.3. Enzymatic Properties of saPLD@NFs

As demonstrated in Figure 4a, the optimal temperatures of both saPLD@NFs and free saPLD were 60 °C. However, the relative activity of saPLD@NFs was greater than that of free saPLD in the range of 30–80 °C. Figure 4b exhibits that saPLD@NFs retained more residual activity than free saPLD when incubating from 30 to 60 °C. After 1 h incubation at 30 °C and 40 °C, free saPLD retained 101.0% and 72.6% of its original activity, respectively, while saPLD@NFs retained approximately 104.0% and 98.9% of its original activity. Furthermore, free saPLD only retained approximately 5.5% and 1.3% of the original activity after incubating at 50 °C and 60 °C for 1 h, respectively. But saPLD@NFs were more stable, retaining about 59.7% and 31.5% of the original activity, suggesting that the thermostability of saPLD was elevated by an enzyme-inorganic hybrid nanoflowers system.

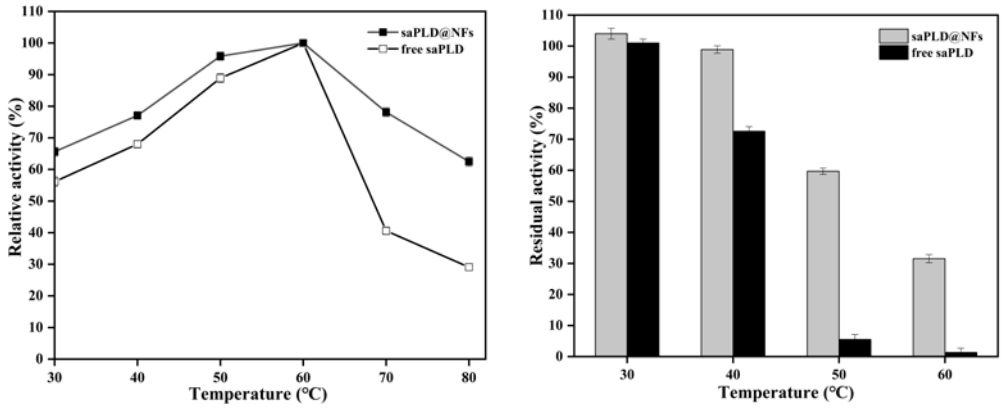

(**a**) (**b**)

Figure 4. Influence of temperature on the activity (**a**) and stability (**b**) of saPLD@NFs and free saPLD. The data exhibited are the average values obtained from three paralleled experiments, while the error bars stand for the standard deviations.

As exhibited in Figure 5a, the optimal pH values of saPLD@NFs and free saPLD were the same, demonstrating their maximum activities at pH 6.0. However, saPLD@NFs showed greater relative activities in the range of pH 5.0–9.0 in comparison to free saPLD. As demonstrated in Figure 5b, the residual activity of saPLD@NFs was 94.4%, 99.6%, 95.0%,

and 86.1% after 7 d incubation at pH 5.0, 6.0, 7.0, and 8.0, respectively, while free saPLD retained 86.7%, 91.7%, 87.8%, and 81.7% of its original activity under the respective pH conditions. This indicated that the pH stability of saPLD was enhanced by the application of the enzyme-inorganic hybrid nanoflowers system.

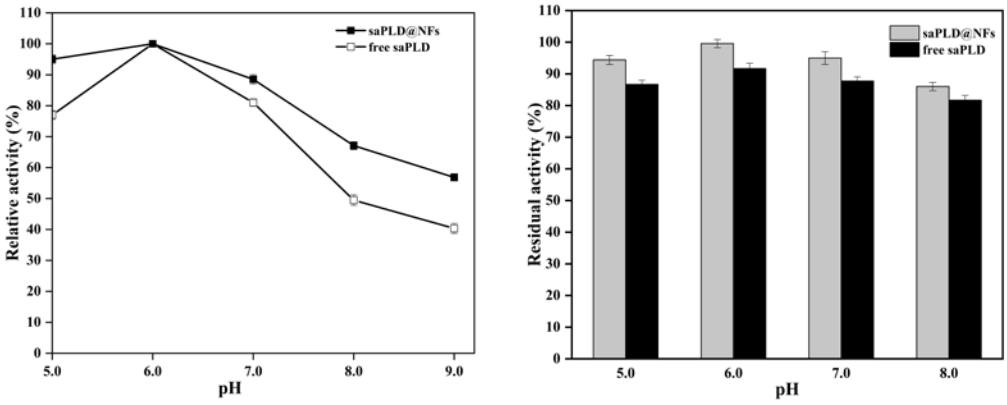

(**a**) (**b**)

Figure 5. Influence of pH on the activity (**a**) and stability (**b**) of saPLD@NFs and free saPLD. The data exhibited are the average values obtained from three paralleled experiments, while the error bars stand for the standard deviations.

The improved thermostability and pH stability of saPLD@NFs were considered to be caused by the saPLD molecules trapped in nano-porous structures, which increased the enzyme rigidity. The results were mostly in agreement with most of the cases mentioned in the literature, in which the immobilized enzyme demonstrated better stability in comparison to the free enzyme. For example, lipase-inorganic hybrid nanoflowers were synthesized with $Ca_3(PO_4)_2$ as the inorganic component and lipase as the organic component [43], and the ChT-inorganic hybrid nanoflowers were prepared at room temperature in aqueous solution using $Ca_3(PO_4)_2$ as the inorganic component and ChT as the organic component [44], which both exhibited better stability. The outstanding thermostability and pH stability of saPLD@NFs were beneficial for the practical utilization in the functional phospholipid production.

3.4. Synthesis of PS by saPLD@NFs

Given the importance of PS in pharmaceutical and functional food production, the catalytic behavior of saPLD@NFs was analyzed with the reaction between L-serine and PC as the model reaction system (Figure 6). Over the years, PS synthesis with L-serine and PC by PLD-mediated transphosphatidylation has been frequently reported, and the organic-water biphasic reaction system was the most extensively studied and performed [45]. Although PS has been synthesized using numerous organic solvents, including chloroform, toluene, and diethyl ether, with a maximal yield of ~95%, organic solvents might not be suitable for the food industry due to the possible toxic compounds. Thus, it was essential to develop a reaction system with green and non-toxic ingredients for synthesizing safe PS to apply in functional foods. In this work, PC was dissolved in propyl propionate, which is less toxic than chloroform, diethyl ether, and toluene, and it is utilized as a solvent for perfume and food additives, as well as inks and paints, generally thought to be one of the best environmental options [46].

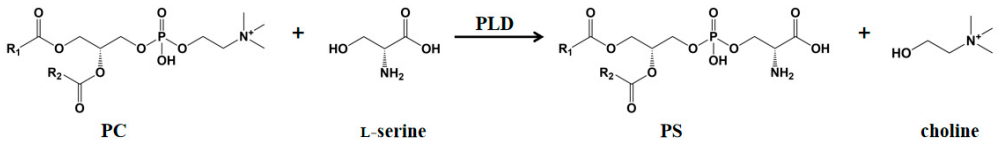

Figure 6. The transphosphatidylation of the PLD.

To optimize the PS yield, variables including the saPLD@NFs amount and reaction time were investigated systematically at 40 °C and pH 6.0 in a propyl propionate-aqueous system according to the characteristics of saPLD@NFs. The enzymatic reaction needed to be carried out under suitable temperature. Although a higher temperature may increase the diffusion behavior of the substrate and decrease the viscosity of the reaction system to enhance the enzyme activity, it might cause enzyme inactivation. saPLD@NFs exhibited a slightly lower activity at 40 °C than 60 °C but demonstrated a better stability at 40 °C than 60 °C, which was of great help to maintain its activity for an extended time. Hence, 40 °C and pH 6.0 were chosen as the parameters for the following experiments.

Figure 7 demonstrates the effect of the saPLD@NFs amount and reaction time on the PS yield. When 0.25 g of saPLD@NFs was added into the reaction system, the PS yield reached 42.6% after 5 h reaction. When 0.50 g and 0.75 g of saPLD@NFs were added to the reaction system, the PS yield was increased from 0 to the maximum of 57.4% and 57.1%, with the reaction time extended from 0 to 3 h, respectively, and then kept stable. The rate of catalytic reaction was directly associated with the quantity of enzyme. The effective collision probability of the enzyme molecule and substrate was enhanced with the increased enzyme amount, leading to a faster reaction speed. When the enzyme molecule quantity was enhanced to a certain extent in the reaction system, the contact of the substrates and enzyme molecules was saturated, resulting in the highest enzymatic reaction speed. Therefore, the optimum saPLD@NFs amount of 0.50 g and reaction time of 3 h were selected to increase the reaction efficiency. To our knowledge, this is the first report to produce PS in an organic-water biphasic reaction system using PLD-synthesized enzyme-inorganic hybrid nanoflowers, which might promote the practical utilization of this biocatalyst.

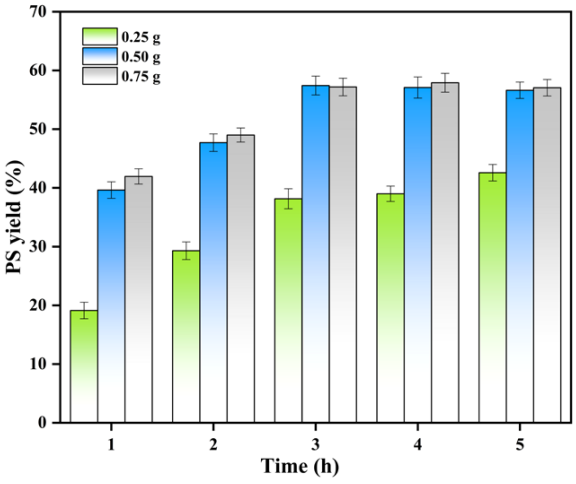

Figure 7. Enzymatic catalysis with different reaction times and enzyme amount. The data exhibited are the average values obtained from three paralleled experiments, while the error bars stand for the standard deviations.

3.5. Storage Stability of saPLD@NFs

Figure 8 shows the time-dependent residual activities of saPLD@NFs and free saPLD. After 25 d incubation, the residual activity of free saPLD gradually decreased to only 38.3%, whereas saPLD@NFs retained 66.5% of the original activity under the same reaction conditions. The greater storage stability of saPLD@NFs might be caused by the excellent

stability of calcium phosphate and the encapsulation of saPLD in the nanoflowers, which hindered its leakage. This suggested that enzyme-inorganic hybrid nanoflowers are highly stable in a chemical environment. The enhanced storage stability facilitated the utilization of saPLD@NFs for synthesizing functional phospholipids.

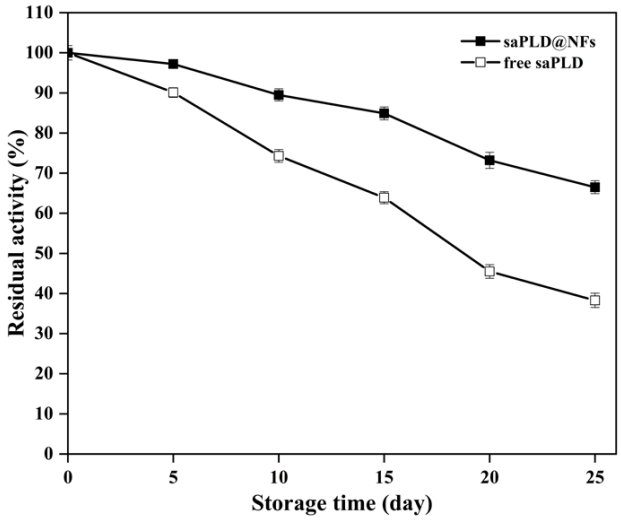

Figure 8. Storage stability of saPLD@NFs and free saPLD. The data exhibited are the average values obtained from three paralleled experiments, while the error bars stand for the standard deviations.

3.6. Operational Stability of saPLD@NFs

Operational stability plays an essential role in decreasing the operating cost in practical applications but the difficulty in reutilizing free PLDs leads to the high cost of the enzymatic process. The reusability of immobilized PLDs is an important criterion for their cost-effective usage and industrial application. Therefore, it is essential to explore immobilized PLDs for reutilizing in their practical application of producing PS. As presented in Figure 9, the PS yield was approximately 57.4% in the first cycles and still retained 60.4% of its initial value after four cycles. Hence, saPLD@NFs could be reutilized over four times from a practical perspective. The decreased PS yield with cycle times should be mostly due to the deactivated saPLD@NFs after the continuous catalytic operations. Furthermore, the loss of saPLD@NFs due to the repeated washing and centrifugation was another reason, which was similar to the previously reported laccase-loaded magnetic nanoflowers [38]. In summary, saPLD@NFs are a potential biocatalyst for producing functional phospholipids in an inexpensive approach.

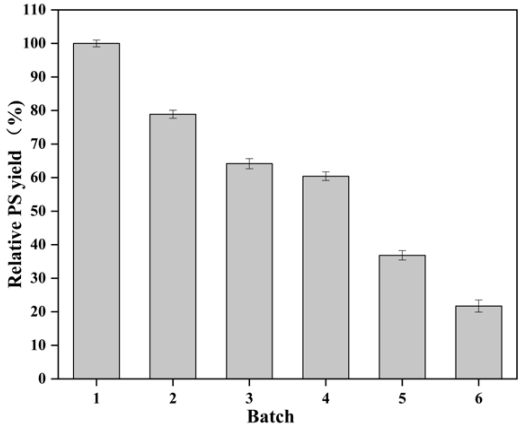

Figure 9. Operational stability of saPLD@NFs. The data exhibited are the average values obtained from three paralleled experiments, while the error bars stand for the standard deviations.

4. Conclusions

Nowadays, lots of attention has been paid to the enzyme-inorganic hybrid nanoflowers due to their high activity, good stability, simple synthesis, and low cost. In this work, saPLD@NFs were successfully prepared using saPLD as the organic component and $Ca_3(PO_4)_2$ as the inorganic component. The optimum immobilization condition for saPLD was obtained by investigating the Ca^{2+} concentration and enzyme content of hybrid nanoflowers. Compared to free saPLD, the synthesized saPLD@NFs demonstrated outstanding performance, with an active enzyme recovery rate of 119%. Additionally, saPLD@NFs exhibited better thermostability and pH stability than free saPLD, suggesting the potential of saPLD@NFs for PS production as a new kind of biocatalyst. It also showed higher storage stability than free saPLD and retained greater residual activities after 25 d incubation. Furthermore, the PS yield of saPLD@NFs was 57.4%, and the relative yield was still over 60% after four consecutive batches in the organic-water biphasic reaction system, indicating its suitability for practical production applications. In summary, saPLD@NFs and the related reaction system would establish a novel approach for the effective production of PS.

Supplementary Materials: The following supporting information can be downloaded at: https://www.mdpi.com/article/10.3390/fermentation9121016/s1. Figure S1: HPLC standard curve of PS concentration; Table S1: The influence of enzyme content and Ca^{2+} concentration on the relative enzyme activity and the enzyme activity recovery rate; Table S2: Influence of temperature on the activity of saPLD@NFs and free saPLD; Table S3: Influence of temperature on the stability of saPLD@NFs and free saPLD; Table S4: Influence of pH on the activity of saPLD@NFs and free saPLD; Table S5: Influence of pH on the stability of saPLD@NFs and free saPLD; Table S6: Enzymatic catalysis with different reaction times and enzyme amount.

Author Contributions: Conceptualization, S.Z. and H.S.; methodology, S.Z., H.S. and Z.H. (Zhuoxuan Han); formal analysis, S.Z., H.S., Z.H. (Zhiqi Huang), Z.H. (Zhuoxuan Han) and J.H.; investigation, S.Z., H.S., Z.H. (Zhiqi Huang), Z.H. (Zhuoxuan Han) and J.H.; writing—original draft preparation, S.Z. and H.S.; writing—review and editing, F.L. and Y.L.; supervision, Y.L.; project administration, Y.L.; funding acquisition, Y.L. All authors have read and agreed to the published version of the manuscript.

Funding: This work was supported by the National Natural Science Fund of China (32172156), the National Key Research and Development Program of China (2021YFC2100300), and the Tianjin Key-Training Program of "Project and Team" of China (XC202032).

Institutional Review Board Statement: Not applicable.

Informed Consent Statement: Not applicable.

Data Availability Statement: The data presented in this study are available on request from the corresponding author.

Conflicts of Interest: The authors declare no conflict of interest.

References

1. Liu, Y.; Huang, L.; Fu, Y.; Zheng, D.; Ma, J.; Li, Y.; Xu, Z.; Lu, F. A novel process for phosphatidylserine production using a *Pichia pastoris* whole-cell biocatalyst with overexpression of phospholipase D from *Streptomyces halstedii* in a purely aqueous system. *Food Chem.* **2019**, *274*, 535–542. [CrossRef] [PubMed]
2. Sun, H.; Zhang, S.; Liu, D.; Huang, Z.; Ge, Y.; Hou, J.; Lu, F.; Liu, Y. Immobilization of Phospholipase D for Production of Phosphatidylserine by a Pickering Emulsion Strategy. *Catalysts* **2023**, *13*, 1318. [CrossRef]
3. Yin, C.; Zhang, H.; Mao, X. Cellulose nanofibril-stabilized Pickering emulsion as a high-performance interfacial biocatalysis system for the synthesis of phosphatidylserine. *Food Chem.* **2023**, *399*, 133865. [CrossRef] [PubMed]
4. Zhang, Y.Y.; Yang, L.Q.; Guo, L.M. Effect of phosphatidylserine on memory in patients and rats with Alzheimer's disease. *Genet. Mol. Res.* **2015**, *14*, 9325–9333. [CrossRef] [PubMed]
5. Kim, H.Y.; Huang, B.X.; Spector, A.A. Phosphatidylserine in the brain: Metabolism and function. *Prog. Lipid Res.* **2014**, *56*, 1–18. [CrossRef] [PubMed]
6. Glade, M.J.; Smith, K. Phosphatidylserine and the human brain. *Nutrition* **2015**, *31*, 781–786. [CrossRef] [PubMed]
7. Starks, M.A.; Starks, S.L.; Kingsley, M.; Purpura, M.; Jager, R. The effects of phosphatidylserine on endocrine response to moderate intensity exercise. *J. Int. Soc. Sports Nutr.* **2008**, *5*, 11. [CrossRef]

8. Liu, Y.; Zhang, T.; Qiao, J.; Liu, X.; Bo, J.; Wang, J.; Lu, F. High-yield phosphatidylserine production via yeast surface display of phospholipase D from *Streptomyces chromofuscus* on *Pichia pastoris*. *J. Agric. Food Chem.* **2014**, *62*, 5354–5360. [CrossRef]
9. Li, M.; Zhou, Y.; Duan, X.; Zhou, L.; Zhang, T. Characterization of a phospholipase D from *Streptomyces cinnamoneum* SK43.003 suitable for phosphatidylserine synthesis. *Biotechnol. Appl. Biochem.* **2022**, *69*, 1917–1928. [CrossRef]
10. Hou, H.J.; Gong, J.S.; Dong, Y.X.; Qin, J.; Li, H.; Li, H.; Lu, Z.M.; Zhang, X.M.; Xu, Z.H.; Shi, J.S. Phospholipase D engineering for improving the biocatalytic synthesis of phosphatidylserine. *Bioprocess. Biosyst. Eng.* **2019**, *42*, 1185–1194. [CrossRef]
11. Morris, A.J.; Engebrecht, J.; Frohman, M.A. Structure and regulation of phospholipase D. *Trends Pharmacol. Sci.* **1996**, *17*, 182–185. [CrossRef] [PubMed]
12. Imamura, S.; Horiuti, Y. Purification of *Streptomyces chromofuscus* phospholipase D by hydrophobic affinity chromatography on palmitoyl cellulose. *J. Biochem.* **1979**, *85*, 79–95. [CrossRef] [PubMed]
13. Yu, C.H.; Liu, S.Y.; Panagia, V. The transphosphatidylation activity of phospholipase D. *Mol. Cell Biochem.* **1996**, *157*, 101–105. [CrossRef] [PubMed]
14. Damnjanovic, J.; Iwasaki, Y. Phospholipase D as a catalyst: Application in phospholipid synthesis, molecular structure and protein engineering. *J. Biosci. Bioeng.* **2013**, *116*, 271–280. [CrossRef] [PubMed]
15. Yang, S.F.; Freer, S.; Benson, A.A. Transphosphatidylation by Phospholipase D. *J. Biol. Chem.* **1967**, *242*, 477–484. [CrossRef] [PubMed]
16. Stanacev, N.Z.; Stuhne-Sekalec, L. On the mechanism of enzymatic phosphatidylation. Biosynthesis of cardiolipin catalyzed by phospholipase D. *Biochim. Biophys. Acta* **1970**, *210*, 350–352. [CrossRef] [PubMed]
17. Veronese, F.M. Peptide and protein PEGylation: A review of problems and solutions. *Biomaterials* **2001**, *22*, 405–417. [CrossRef]
18. Zhang, Y.-T.; Zhi, T.-T.; Zhang, L.; Huang, H.; Chen, H.-L. Immobilization of carbonic anhydrase by embedding and covalent coupling into nanocomposite hydrogel containing hydrotalcite. *Polymer* **2009**, *50*, 5693–5700. [CrossRef]
19. Romero-Arcos, M.; Pérez-Robles, J.F.; Guadalupe Garnica-Romo, M.; Luna-Martinez, M.S.; Gonzalez-Reyna, M.A. Synthesis and functionalization of carbon nanotubes and nanospheres as a support for the immobilization of an enzyme extract from the mushroom *Trametes versicolor*. *J. Mater. Sci.* **2019**, *54*, 11671–11681. [CrossRef]
20. Wang, M.; Qi, W.; Su, R.; He, Z. Advances in carrier-bound and carrier-free immobilized nanobiocatalysts. *Chem. Eng. Sci.* **2015**, *135*, 21–32. [CrossRef]
21. Zhou, Z.; Hartmann, M. Progress in enzyme immobilization in ordered mesoporous materials and related applications. *Chem. Soc. Rev.* **2013**, *42*, 3894–3912. [CrossRef] [PubMed]
22. Cui, J.; Ren, S.; Lin, T.; Feng, Y.; Jia, S. Shielding effects of Fe^{3+}-tannic acid nanocoatings for immobilized enzyme on magnetic Fe_3O_4@silica core shell nanosphere. *Chem. Eng. J.* **2018**, *343*, 629–637. [CrossRef]
23. Sun, J.; Yendluri, R.; Liu, K.; Guo, Y.; Lvov, Y.; Yan, X. Enzyme-immobilized clay nanotube-chitosan membranes with sustainable biocatalytic activities. *Phys. Chem. Chem. Phys.* **2016**, *19*, 562–567. [CrossRef] [PubMed]
24. Xu, X.; Qi, X.; Wang, X.; Wang, X.; Wang, Q.; Yang, H.; Fu, Y.; Yao, S. Highly efficient enzyme immobilization by nanocomposites of metal organic coordination polymers and carbon nanotubes for electrochemical biosensing. *Electrochem. Commun.* **2017**, *79*, 18–22. [CrossRef]
25. Cui, J.; Lin, T.; Feng, Y.; Tan, Z.; Jia, S. Preparation of spherical cross-linked lipase aggregates with improved activity, stability and reusability characteristic in water-in-ionic liquid microemulsion. *J. Chem. Technol. Biotechnol.* **2017**, *92*, 1785–1793. [CrossRef]
26. Liu, X.; Fang, Y.; Yang, X.; Li, Y.; Wang, C. Electrospun epoxy-based nanofibrous membrane containing biocompatible feather polypeptide for highly stable and active covalent immobilization of lipase. *Colloids Surf. B Biointerfaces* **2018**, *166*, 277–285. [CrossRef]
27. Ding, S.; Cargill, A.A.; Medintz, I.L.; Claussen, J.C. Increasing the activity of immobilized enzymes with nanoparticle conjugation. *Curr. Opin. Biotechnol.* **2015**, *34*, 242–250. [CrossRef]
28. Ge, J.; Lu, D.; Liu, Z.; Liu, Z. Recent advances in nanostructured biocatalysts. *Biochem. Eng. J.* **2009**, *44*, 53–59. [CrossRef]
29. Soni, S.; Dwivedee, B.P.; Banerjee, U.C. An Ultrafast Sonochemical Strategy to Synthesize Lipase-Manganese Phosphate Hybrid Nanoflowers with Promoted Biocatalytic Performance in the Kinetic Resolution of β-Aryloxyalcohols. *ChemNanoMat* **2018**, *4*, 1007–1020. [CrossRef]
30. Zhang, M.; Zhang, Y.; Yang, C.; Ma, C.; Tang, J. Enzyme-inorganic hybrid nanoflowers: Classification, synthesis, functionalization and potential applications. *Chem. Eng. J.* **2021**, *415*, 129075. [CrossRef]
31. Ge, J.; Lei, J.; Zare, R.N. Protein-inorganic hybrid nanoflowers. *Nat. Nanotechnol.* **2012**, *7*, 428–432. [CrossRef] [PubMed]
32. Shi, J.; Zhang, S.; Wang, X.; Yang, C.; Jiang, Z. Preparation and enzymatic application of flower-like hybrid microcapsules through a biomimetic mineralization approach. *J. Mater. Chem. B* **2014**, *2*, 4289–4296. [CrossRef] [PubMed]
33. Wang, L.; Li, F.; Wang, S.; Wu, J.; Zhang, W.; Zhang, Y.; Liu, W. Time-temperature indicators based on Lipase@$Cu_3(PO_4)_2$ hybrid nanoflowers. *LWT* **2022**, *168*, 113857. [CrossRef]
34. Lin, Z.; Xiao, Y.; Wang, L.; Yin, Y.; Zheng, J.; Yang, H.; Chen, G. Facile synthesis of enzyme–inorganic hybrid nanoflowers and their application as an immobilized trypsin reactor for highly efficient protein digestion. *RSC Adv.* **2014**, *4*, 13888–13891. [CrossRef]
35. Hao, Y.; Li, H.; Cao, Y.; Chen, Y.; Lei, M.; Zhang, T.; Xiao, Y.; Chu, B.; Qian, Z. Uricase and Horseradish Peroxidase Hybrid $CaHPO_4$ Nanoflower Integrated with Transcutaneous Patches for Treatment of Hyperuricemia. *J. Biomed. Nanotechnol.* **2019**, *15*, 951–965. [CrossRef] [PubMed]

36. Lee, I.; Cheon, H.J.; Adhikari, M.D.; Tran, T.D.; Yeon, K.M.; Kim, M.I.; Kim, J. Glucose oxidase-copper hybrid nanoflowers embedded with magnetic nanoparticles as an effective antibacterial agent. *Int. J. Biol. Macromol.* **2020**, *155*, 1520–1531. [CrossRef] [PubMed]
37. Somturk, B.; Yilmaz, I.; Altinkaynak, C.; Karatepe, A.; Ozdemir, N.; Ocsoy, I. Synthesis of urease hybrid nanoflowers and their enhanced catalytic properties. *Enzym. Microb. Technol.* **2016**, *86*, 134–142. [CrossRef] [PubMed]
38. Fu, M.; Xing, J.; Ge, Z. Preparation of laccase-loaded magnetic nanoflowers and their recycling for efficient degradation of bisphenol A. *Sci. Total Environ.* **2019**, *651*, 2857–2865. [CrossRef]
39. Yu, Y.; Fei, X.; Tian, J.; Xu, L.; Wang, X.; Wang, Y. Self-assembled enzyme-inorganic hybrid nanoflowers and their application to enzyme purification. *Colloids Surf. B Biointerfaces* **2015**, *130*, 299–304. [CrossRef]
40. Zhang, B.; Li, P.; Zhang, H.; Fan, L.; Wang, H.; Li, X.; Tian, L.; Ali, N.; Ali, Z.; Zhang, Q. Papain/$Zn_3(PO_4)_2$ hybrid nanoflower: Preparation, characterization and its enhanced catalytic activity as an immobilized enzyme. *RSC Adv.* **2016**, *6*, 46702–46710. [CrossRef]
41. Mao, S.; Zhang, Z.; Ma, X.; Tian, H.; Lu, F.; Liu, Y. Efficient secretion expression of phospholipase D in *Bacillus subtilis* and its application in synthesis of phosphatidylserine by enzyme immobilization. *Int. J. Biol. Macromol.* **2021**, *169*, 282–289. [CrossRef] [PubMed]
42. Lou, L.; Li, Z.; Li, Z. Rational Design to Enhance Enzyme Activity for the Establishment of an Enzyme-Inorganic Hybrid Nanoflower Co-Immobilization System for Efficient Nucleotide Production. *J. Agric. Food Chem.* **2022**, *70*, 2312–2319. [CrossRef] [PubMed]
43. Li, C.; Zhao, J.; Zhang, Z.; Jiang, Y.; Bilal, M.; Jiang, Y.; Jia, S.; Cui, J. Self-assembly of activated lipase hybrid nanoflowers with superior activity and enhanced stability. *Biochem. Eng. J.* **2020**, *158*, 107582. [CrossRef]
44. Yin, Y.; Xiao, Y.; Lin, G.; Xiao, Q.; Lin, Z.; Cai, Z. An enzyme-inorganic hybrid nanoflower based immobilized enzyme reactor with enhanced enzymatic activity. *J. Mater. Chem. B* **2015**, *3*, 2295–2300. [CrossRef]
45. Damnjanović, J.; Iwasaki, Y. Enzymatic Modification of Phospholipids by Phospholipase D. In *Lipid Modification by Enzymes and Engineered Microbes*; AOCS Press: Champaign, IL, USA, 2018; pp. 69–88. [CrossRef]
46. Nogueira, I.B.R.; Faria, R.P.V.; Rodrigues, A.E.; Loureiro, J.M.; Ribeiro, A.M. Chromatographic studies of n-Propyl Propionate, Part II: Synthesis in a fixed bed adsorptive reactor, modelling and uncertainties determination. *Comput. Chem. Eng.* **2019**, *128*, 164–173. [CrossRef]